

Advances in Vibrationally Resonant Sum-Frequency Generation Microscopy

Eric O. Potma

University of California, Irvine, Department of Chemistry, Natural Sciences II, Irvine, CA 92697, USA
epotma@uci.edu

Abstract: Vibrationally resonant sum-frequency generation microscopy is a member of the family of nonlinear optical microscopy techniques. It enables chemically selective imaging of non-centrosymmetric structures. We present the latest advances in this field.

OCIS codes: 180.4315, 190.4223

1. The emerging field of sum-frequency generation microscopy

Second-harmonic generation (SHG) is a second-order optical effect, which is sensitive to the presence of non-centrosymmetrically arranged molecular structures. Since the 1990s, SHG microscopy rapidly ascended as a method for visualizing key structural protein complexes in tissues and cells [1, 2]. Facilitated by the production of commercial SHG imaging modalities, the technique has become a staple of the nonlinear optical imaging approach and has found its way into many research laboratories worldwide. Applications range from the visualization of collagen in numerous tissues such as skin, bone, tendon, lung, liver and kidneys, to the imaging of myosin complexes in muscles and microtubules in individual cells.

Yet, the contrast in standard SHG microscopy is not spectroscopic in nature. Virtually all SHG imaging studies are based on the use of a near-infrared light source such as a Ti:sapphire laser, which produces a nonresonant SHG signal in biological materials. Under these conditions, the signal contains information about the spatial organization of the structures, but its nonresonant character is unspecific about which part of the molecule contributes to the detected signal. In the case of collagen I, many studies have been devoted to connect the polarization properties of the SHG signal to the orientation of particular chemical groups. Despite the numerous publications on SHG imaging of collagen and other structures, a direct relation between the nonlinear signal and the molecular structure remains obscure, because SHG is not chemically selective.

Sum-frequency generation (SFG), is a technique related to SHG with the important exception that SFG can be operated under vibrationally resonant conditions. SFG spectroscopy employs two laser beams, one in the visible/NIR range (ω_{vis}), and another in the mid-IR range (ω_{IR}). Vibrational resonance is achieved when ω_{IR} is close to the frequency of a molecular mode with the proper symmetry. The signal is detected at $\omega_{SFG} = \omega_{IR} + \omega_{vis}$, which is typically in the visible range of the spectrum, and can thus be easily observed with conventional photomultiplier tubes. Similar to SHG, SFG probes the second-order nonlinear susceptibility $\chi^{(2)}$, but because SFG can be tuned into selected vibrational resonances, the second-order response can be assigned to specific chemical groups of the molecule. It is clear that SFG spectroscopic contrast would complement the existing contrast in a nonlinear, multi-modal optical microscope.

Several attempts have been made to design an excitation and detection configuration for efficient SFG microscopic imaging. Inspired by the configuration used in SFG spectroscopy experiments, the first SFG microscopes were based on wide-field illumination (illumination area is hundreds of μm^2) of the sample, where the SFG radiation is captured by a high numerical aperture (NA) lens to form an image on a camera [3]. However, modern nonlinear optical (NLO) imaging techniques, such as SHG, two-photon excited fluorescence (TPEF) and coherent Raman scattering (CRS) microscopy, are based on laser scanning technologies to rapidly acquire images. In addition, NLO microscopes are driven by high-repetition rate ultrafast lasers, which are user-friendly and exhibit an optimized balance between peak power and average power for rapid imaging. On the other hand, most SFG microscopes to date have used amplified laser systems, whose low repetition rates are not optimized for laser scanning microscopy. [4–6] Unfortunately, the combination of non-ideal light sources and incompatible excitation schemes has contributed to the perception that SFG microscopy is not suitable for high-resolution, fast laser-scanning imaging applications.

2. Recent advances

The applicability of SFG imaging depends on its ease of use and its compatibility with existing multi-modal NLO microscopes. A step in this direction was made in 2011, by using a picosecond synchronously-pumped optical parametric oscillator (OPO) as the light source, which produces high repetition rate radiation in the 2800–3100 cm^{-1} range. Adopting a collinear excitation geometry, it was shown that fast SFG imaging can be achieved with an unprecedented lateral resolution of 0.6 μm without computational image enhancement [7] A layout of this SFG microscope is shown in Figure 1a. The collinear SFG microscope produces signals that are comparable in magnitude to the SHG signal or the CRS signal in NLO microscopy. In addition, collinear focusing enables multi-modal, nonlinear optical imaging. In Figure 1b,c, SHG and SFG images of collagen are shown that were simultaneously acquired. SFG uniquely probes vibrational modes with combined IR and Raman activity in $\chi^{(2)}$ -active materials, whereas coherent Raman scattering (CRS) visualizes materials based on $\chi^{(3)}$ and exclusively probes Raman-active vibrational transitions. [8] Hence, the SFG and CRS techniques complement each other, offering the microscopist a rich palette of unique contrast mechanisms.

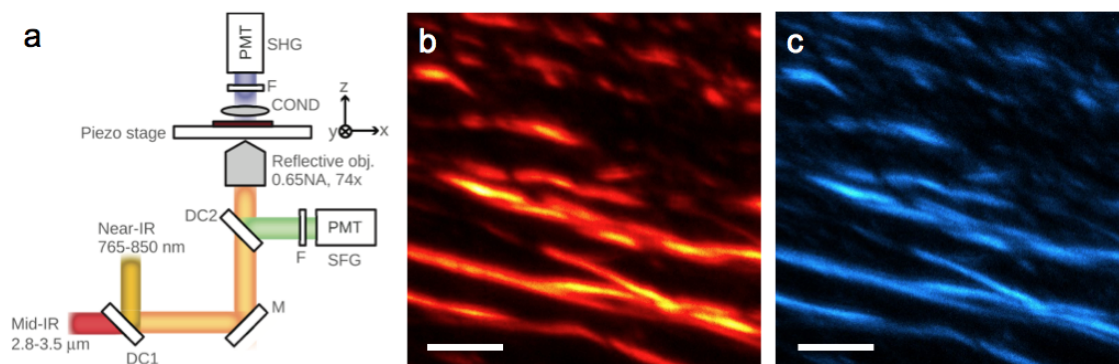


Fig. 1. Collinear SFG microscopy with a high-repetition rate light source. a) Layout of the SFG microscope. DC: dichroic mirror; M: reflecting mirror; F: bandpass filter. COND: condenser; PMT: photomultiplier tube. b) Epi-SFG image of collagen from hawk cornea at 2945 cm^{-1} (CH stretch). c) Forward-SHG image of the same cornea sample. Scale bar is 20 μm .

Recent advances include the implementation of phase-sensitive detection [9], which enables a direct view of chemical group orientation of molecular compounds in tissue, and the use of polarization sensitive SFG [10], which allows a detailed examination of the tensorial properties of $\chi^{(2)}$ -active materials in the tissue. Although these applications demonstrate the utility of SFG microscopy, several technical challenges remain. Vibrationally sensitive SFG relies on the use of coherent mid-IR radiation. Conventional microscope optics and imaging systems are generally not optimized for guiding laser beams in both the visible range as well as in the mid-IR range. This translates into sub-optimal focusing optics, which prevent focusing properties similar to what can be achieved with visible/near-IR optics. The scanning mirrors used in fast-scanning nonlinear optical microscopes rely on an achromatic scan lens and a tube lens for redirecting the laser beam from the scanner to the back aperture of the objective lens. A reflective-based lens system cannot always be used because the geometrical constraints imposed by standard microscope frames, and the lack of achromatic refractive optics for SFG imaging complicates the implementation of galvanometric laser scanners. This has precluded real-time imaging capabilities in SFG microscopy, and significantly held back the practical use of the technique.

To address these issues, we have designed and fabricated new scan and tube lenses, which enable achromatic imaging and focusing from the visible to the mid-infrared range. These lenses make it possible to use standard galvanometric scanners and microscope frames for SFG imaging in a multi-modal NLO configuration. In addition, we have also examined refractive objective lens systems, which make it possible to generate sub- μm resolution images without the use of reflective optics [11]. Furthermore, we have used a picosecond Yb-fiber laser and a new, improved design of the OPO, delivering tunable radiation in the 2.5 to 4.5 μm range. These improvements make it possible to acquire simultaneous SFG, SHG and CRS images at frames rates of 1 image/s. We will present and discuss imaging results on tissues, including cornea and tendon tissues, using the improved imaging capabilities.

References

1. P. J. Campagnola, C. Y. Dong, "Second harmonic generation microscopy: principles and applications to disease diagnosis," *Laser & Photonics Reviews* **5**, 13–26 (2011).
2. F. S. Pavone, P. J. Campagnola, eds., *Second Harmonic Generation Imaging* (CRC Press, Boca Raton, 2013).
3. K. A. Cimatu, S. Baldelli, "Chemical microscopy of surfaces by sum frequency generation imaging," *J. Phys. Chem. C* **113**, 16575–16588 (2009).
4. M. Fl orsheimer, C. Brillert, H. Fuchs, "Chemical imaging of interfaces by sum frequency microscopy," *Langmuir* **15**, 5437–5439 (1999).
5. K. Kuhnke, D. M. P. Hoffmann, X. C. Wu, A. M. Bittner, K. Kern, "Chemical imaging of interfaces by sum-frequency generation microscopy: application to patterns self-assembled monolayers," *Appl. Phys. Lett.* **83**, 3830–3832 (2003).
6. K. Cimatu, S. Baldelli, "Sum frequency generation microscopy of microcontact-printed mixed self-assembled monolayers," *J. Phys. Chem. B* **110**, 1807–1813 (2006).
7. V. Raghunathan, Y. Han, O. Korth, N. H. Ge, E. O. Potma, "Rapid vibrational imaging with sum frequency generation microscopy," *Opt. Lett.* **36**, 3891–3893 (2011).
8. C. Y. Chung, J. C. Boik, E. O. Potma, "Biomolecular imaging with coherent nonlinear vibrational microscopy," *Annu. Rev. Anal. Chem.* **64**, 77–99 (2013).
9. Y. Han, V. Raghunathan, R. Feng, H. Maekawa, C. Y. Chung, Y. Feng, E. O. Potma, N. H. Ge, "Mapping molecular orientation with phase sensitive vibrationally resonant sum-frequency generation microscopy," *J. Phys. Chem. B* **117**, 6149–6156 (2013).
10. Y. Han, J. Hsu, N. H. Ge, and E. O. Potma, "Polarization-sensitive sum-frequency generation microscopy of collagen fibers," *J. Phys. Chem. B* **119**, 3356–3365 (2015).
11. E. S. Lee, S. W. Lee, J. Hsu, E. O. Potma, "Vibrationally resonant sum-frequency generation microscopy with a solid immersion lens," *Biomed. Opt. Express* **5**, 2125–2134 (2014).